TROPHOSOME ULTRASTRUCTURE AND THE CHARACTERIZATION OF ISOLATED BACTERIOCYTES FROM INVERTEBRATE-SULFUR BACTERIA SYMBIOSES

STEVEN C. HAND

Department of Environmental, Population and Organismic Biology, University of Colorado, Campus Box B-334, Boulder, Colorado 80309, and Department of Biology, University of Southwestern Louisiana, Lafayette, Louisiana 70504

ABSTRACT

Electron microscopy of trophosome tissue from the vestimentiferan tubeworm *Riftia pachyptila* clearly indicates that the bacterial symbionts are enclosed within animal cells (bacteriocytes). The structure of this lobular tissue is complex. Each lobule consists of an outer layer of trophochrome cells (devoid of symbionts, but with numerous pigmented granules), an inner region of bacteriocytes, and a central hemolymph space. Sulfur deposits within bacteria decrease in size and number with increasing distance of the bacteria from the hemolymph space. Bacteria located toward the center of the lobule appear smaller than those nearer the periphery, suggesting that metabolic and developmental gradients exist. Trophochrome cells and free bacteria were enriched from the trophosome of *R. pachyptila.*

A procedure is described for the isolation of bacteriocytes from gill tissue of the bivalves *Calyptogena magnifica* and *Lucina floridana.* Numerous bacteria reside in vacuoles within the bacteriocyte cytoplasm, as do large (5–10 micron), heterogeneous granules. Maximum CO_2 fixation rate at 20°C for bacteriocytes from *C. magnifica* is 13.2 nmoles CO_2/mg protein/h, compared to 21.6 nmoles CO_2/mg protein/h for *L. floridana* bacteriocytes. Fixation by bacteriocytes from *C. magnifica* is inhibited by sulfide, and to a lesser extent thiosulfate, at 0.1–1.0 mM. Thiosulfate increases CO_2 fixation two-fold in *L. floridana* bacteriocytes.

C. magnifica bacteriocytes incubated for 1 h in 0.5 mM sulfide maintain higher intracellular ATP concentrations (3.3 nmoles/million cells; 1.01 mM) than do control cells without sulfide (1.02 nmoles/million cells; 0.31 mM). These results and comparable observations suggest that the identities of exogenous sulfur compounds exploited for chemical energy by the symbiosis may depend on the structural integrity and organization of the experimental preparation.

INTRODUCTION

In symbiosis between sulfur bacteria and marine invertebrates, various metabolic features are critically dependent on the cellular integrity of each participant. To study these characteristics without disrupting cellular structure, we developed a procedure for isolating intact bacteriocytes (eucaryotic cells that contain large numbers of bacterial endosymbionts) from gill tissues of the hydrothermal vent clam, *Calyptogena magnifica,* and the shallow-water bivalve *Lucina floridana,* an inhabitant of seagrass beds. An ultrastructural description of the intact trophosome of the hydrothermal

vent tubeworm *Riftia pachyptila* (Pogonophora) provides new information about cellular arrangements and metabolic potentials in this symbiont-containing tissue. Finally, using bacteriocyte suspensions prepared from the bivalves, we measured intracellular ATP levels and the capacity for carbon fixation in the presence of various sulfur compounds.

The primary advantage of using bacteriocytes for metabolic studies is that the symbiotic bacteria are retained in their natural microenvironment. As a consequence, the bacteria receive chemical signals (sulfur compounds, dissolved gases, etc.) via the cytoplasm of the host cell. Furthermore, all bacteriocyte surfaces are in direct contact with medium constituents, so that the effects of slowly exchanging compartments such as connective tissue spaces are minimized. Thus individual bacteriocytes are considered functional symbiotic units, and their response to various stimuli quantified on a cellular basis.

Until now, isolated invertebrate cells have not been used to study physiological and biochemical relationships between sulfur oxidizing bacteria and the host. Rather, previous studies have focused on other levels of biological organization and complexity. Data have been obtained using (1) the intact symbiosis at the whole-organism level (*e.g.,* Anderson, 1986; Arp *et al.,* 1984; Childress *et al.,* 1984; Felbeck, 1983, 1985; Fiala-Medioni *et al.,* 1986), (2) excised tissues (*e.g.,* Cavanaugh, 1983; Dando *et al.,* 1985; Felbeck, 1983; Powell and Somero, 1983), (3) variously prepared homogenates of tissues (*e.g.,* Felbeck, 1981; Felbeck *et al.,* 1981; Fisher and Childress, 1984; Fisher and Hand, 1984; Hand and Somero, 1983; Powell and Somero, 1985, 1986a), and (4) isolated bacteria and cellular organelles (*e.g.,* Belkin *et al.,* 1986; Powell and Somero, 1986b). Depending on the degree of tissue disruption, significant variation was observed in the metabolism of sulfur compounds and the rates and characteristics of carbon fixation. For example, using homogenates of gill tissue from *C. magnifica,* Powell and Somero (1986b) reported that stimulation of ATP synthesis by sulfur compounds occurred only when bacteria contained therein were lysed.

Experimental preparations that maintain the bacteria in more biologically realistic surroundings offer new opportunities for assessing their metabolic potential. This possibility was the impetus for the present study. In addition to isolating bacteriocytes from gill tissue of *C. magnifica* and *L. floridana,* we isolated trophochrome cells (green pigmented cells) and free bacteria from trophosome tissue of *R. pachyptila.* Although electron micrographs presented herein indicate bacteriocytes within the trophosome, we were unsuccessful in isolating them intact from this source.

MATERIALS AND METHODS

Experimental animals and reagents

Specimens of *Riftia pachyptila* and *Calyptogena magnifica* were collected in March 1985 during the hydrothermal vent expedition to the Galapagos Rift with the submersible DSRV Alvin at the "Rose Garden" site (Hessler and Smithey, 1983). The live animals on board the RV Melville were handled as described by Powell and Somero (1986a). Tissue samples were dissected from specimens of *R. pachyptila* and *C. magnifica* typically within 3 h of their arrival on board ship. Tissue weights were determined with the motion compensated shipboard balance developed by Childress and Mickel (1980).

Specimens of the eulamellibranch bivalve *Lucina floridana* were collected from the sulfide-rich sediments of *Thalassia* and *Ruppia* seagrass beds in St. Joseph's Bay, Florida. Animals were maintained in the laboratory as described by Fisher and Hand (1984) for no more than three weeks prior to tissue dissection.

Hyaluronidase (Type 1-S), collagenase (Type IV), DNAase I (Type IV), chymotrypsin (Type II), soybean trypsin inhibitor, and Percoll were purchased from Sigma Chemical Co. $NaH^{14}CO_3$ was obtained from New England Nuclear. All other chemicals were reagent grade. Solutions of sodium sulfide were prepared fresh before each experiment (Powell and Somero, 1986a) and maintained under nitrogen until use (1–3 h). To reduce mechanical damage to isolated cells, siliconized glassware was used in all steps described below, and all pipets were firepolished.

Tissue dissociation

C. magnifica gill tissue was placed on a chilled glass plate and minced into cubes varying in size from 0.5 mm to 2 mm. The tissue was rinsed briefly in Ca^{++}-Mg^{++} free salt solution (CMF solution) (508 mM NaCl, 10 mM KCl, 8.7 mM $NaHCO_3$, 28.6 mM Na_2SO_4, 0.1 mM EGTA, 4 mM glucose, pH 7.2) to remove mucus. The tissue was then transferred to 50 ml flasks and incubated for 15 min at 20°C in 20 ml of CMF solution on a rotary shaker (110 cycles/min). This initial medium was replaced with 10 ml of artificial seawater (411 mM NaCl, 9.6 mM KCl, 54 mM $MgCl_2$, 10.5 mM $CaCl_2$, 8.8 mM $NaHCO_3$, 23.6 mM Na_2SO_4, glucose 4 mM, pH 7.2) containing hyaluronidase (400 U/ml), collagenase (500 U/ml), and chymotrypsin (70 U/ml), and the tissue was incubated for 1.5 h at 20°C. At the end of this period, the tissue was rinsed with CMF solution and incubated 15 min in 10 ml of CMF solution containing bovine serum albumin (1 mg/ml), trypsin inhibitor (0.4 mg/ml), and DNAase I (15 U/ml). The tissue in this solution was flushed 20–30 times through a siliconized Pasteur pipet, a procedure that released large numbers of cells. The cellular suspension was filtered sequentially through 250 micron and 100 micron nylon mesh (Tetko, Inc.; Elmsford, New York) to remove undissociated tissue.

Isolated cells from *Riftia* trophosome were prepared similarly, except the tissue incubation with enzymes was shortened to one hour at 20°C. The concentrations of enzymes were all reduced 50%, compared to the levels used for *C. magnifica*.

The procedure for dissociation of gill tissue from *L. floridana* differed from the above protocol for *C. magnifica* in several respects. The concentration of the artificial seawater was 40 ppt (470 mM NaCl, 11 mM KCl, 62 mM $MgCl_2$, 12 mM $CaCl_2$, 10 mM $NaHCO_3$, 27 mM Na_2SO_4, 0.1 mM EGTA, 5 mM glucose, pH 7.2), and the CMF solution consisted of 581 mM NaCl, 11.4 mM KCl, 10 mM $NaHCO_3$, 32.7 mM Na_2SO_4, 0.1 mM EGTA, 5 mM glucose, pH 7.2. The minced gill tissue was incubated for 15 min at 37°C in CMF solution, and the concentrations of enzymes used in the subsequent incubation (1 h at 37°C) were 50% of those used for *C. magnifica* tissue.

Cell isolation

The cellular suspension from *C. magnifica* gill was divided into two 5-ml portions, each of which was layered onto a Percoll gradient at 4°C. This gradient separated bacteriocytes from other cell types and from acellular and subcellular debris. Cellular suspensions of *R. pachyptila* trophosome were treated similarly. The 40-ml discontinuous gradient consisted of four steps of 10% (density, 1.042), 30% (1.065), 50% (1.089), and 70% (1.111) Percoll. Each step was prepared by adding appropriate amounts of Percoll and deionized water to 2 ml of a concentrated CMF stock (5×). The cells settled without centrifugation for 3 h at 4°C, and cells that had accumulated at each interface were collected and rinsed twice with artificial seawater to remove Percoll (which interferes with the assay for CO_2 incorporation).

The Percoll gradient was changed to 30%, 50%, 70%, and 90% (density, 1.120) for separation of *L. floridana* bacteriocytes. Each step was prepared in the 40 ppt CMF solution (final concentration).

Cell concentrations were determined with a hemocytometer. The distinguishing features used to identify bacteriocytes under light microscopy were their granular appearance, lack of cilia, and relatively large diameter (20 microns, *C. magnifica;* 40 microns, *L. floridana*).

Transmission electron microscopy

Isolated cells to be fixed for electron microscopy were transferred to Beem capsules and centrifuged at low speed ($500 \times g$) to concentrate the cells. The supernatant was removed, and glutaraldehyde (4% in 0.3 M PIPES buffer, pH 7.2 at room temperature) was layered over the cells. Intact tissue for fixation was dissected into small blocks (1 mm diameter) and placed in plastic specimen trays containing glutaraldehyde solution. After 30–60 min, the glutaraldehyde was removed, and the Beem capsule (or specimen tray) was filled with warmed agar (1.5% in 0.3 M PIPES, pH 7.2). After the agar solidified, the capsules were given three 15-min washes in buffer and then placed in 1% osmium tetroxide (prepared in 0.2 M potassium phosphate buffer, pH 7.4) for 2–3 h. The preparations were washed thoroughly with deionized water, dehydrated in a graded acetone series, and embedded in Spurr's low-viscosity media. All the steps above were completed on board ship. Sections were cut with a Sorvall MT 5000 Ultramicrotome and stained with 4% uranyl acetate followed by lead citrate. Cells were viewed with a Hitachi H-600 electron microscope.

CO_2 fixation studies

Isolated cells (100,000–500,000 for each assay) were incubated for up to 30 min in 0.5 ml of artificial seawater (pH 8.2) containing 1 microcurie of $NaH^{14}CO_3$, with and without various concentrations of sulfide and thiosulfate. All incubations were performed at 20°C. Incorporation of CO_2 was stopped by vigorously mixing 0.1 ml of 12 N HCl with each sample. Samples were transferred to plastic counting vials and heated for 2 h at 90°C. Radioactivity remaining in the acid soluble fraction was quantified with liquid scintillation counting. Values for duplicate samples stopped at time 0 were subtracted from all treatments.

ATP measurements

Experiments to determine the influence of sulfur compounds on cellular ATP levels were performed similarly to those above, but the radioactive bicarbonate was omitted from the incubation medium. At the end of the incubation, cells were sedimented with low speed centrifugation ($500 \times g$, 5 min) at 4°C, and the incubation medium was decanted. Cells were then resuspended in 0.5 ml of ice-cold 0.6 M perchloric acid and homogenized. The homogenate was neutralized (and perchlorate salts precipitated) with 0.15 ml of a solution containing 0.2 N KOH, 0.4 M imidazole, and 0.4 M KCl. The supernatant was initially stored in liquid nitrogen on board ship and later transferred to a −80°C freezer until ATP analyses could be performed.

ATP was measured with an enzyme-coupled fluorometric assay (modified from Lowry and Passonneau, 1972). All solutions were filtered through Gelman TCM-450 (0.45 micron) filters before use. The 1.2 ml assay mixture contained 50 mM Tris-HCl buffer pH 8.1, 1.0 mM MgCl$_2$, 0.2 mM dithiothreitol, 0.05 mM NADP, 0.1 mM glucose, and 50 microliters of sample. First, 0.07 units of glucose-6-phosphate dehy-

drogenase were added to eliminate endogenous G-6-P, and then 0.34 units of hexoki-
nase were added for the quantification of ATP. The excitation wavelength was 365
nm, and the emission monochromator was set at 460 nm. The increase in fluores-
cence was measured with a Turner Model 430 spectrofluorometer, and the fluores-
cence signal was adjusted so that 0.1 nmole of ATP gave a 25% full scale deflection.

Protein measurements

Total protein was analyzed following the procedure of Peterson (1977).

RESULTS

Morphology of trophosome tissue

Fresh trophosome from *R. pachyptila* is a gelatinous, pulpy, dark iridescent-green
tissue. If the tissue is suspended in saline, numerous finger-like lobules project into
the medium producing a villous appearance. Each lobule is approximately 0.15 mm
in diameter and has a complex ultrastructure that is revealed by examining cross
sections with electron microscopy (Fig. 1A).

The cells composing the outer pigmented layer of the lobule are tightly packed
with membrane-bound inclusions of at least three morphological types. One type of
granule (Fig. 1B, 2A) is homogeneous in composition, weakly electron-dense, and
similar in appearance to mucus droplets or mucigen granules found in goblet cells of
intestinal epithelia (*e.g.,* Porter and Bonneville, 1973). In contrast, the darker osmio-
philic granules (Fig. 1B, 2B) contain highly organized, crystalline arrays of material
(probably proteinaceous) that may be responsible for the intense green color of the
trophosome. Indeed, if this outer cellular layer is osmotically lysed and removed from
fresh trophosome tissue, the underlying tissue is white (R. Vetter, pers. comm.). The
third type of inclusion (Fig. 1B) has an electron density intermediate to that of the
previous two granules, and its appearance indicates a heterogeneous composition.
Thus, based on the internal morphology, these pigmented cells comprising the outer
layer of trophosome tissue are referred to hereafter as trophochrome cells.

Nuclei are visible in the trophochrome cells, but other common organelles (*e.g.,*
mitochondria, endoplasmic reticulum) are infrequent. The granules described above
occupy the vast majority of the intracellular space. Even though it is possible that
osmotic swelling could have accentuated the size of these inclusions, the structural
integrity of both the limiting and internal cell membranes does not suggest extensive
swelling.

Subtending the trophochrome cell layer are numerous bacterial endosymbionts
(Fig. 3A, B). The bacteria housed in trophosome tissue are roughly spherical, often
with irregular cell envelopes, and are approximately 3–5 microns in diameter. As one
moves toward the center of the lobule, the morphology of the bacteria changes. Sulfur
deposits within bacteria increase in both size and number, and ribosomes in the bac-
terial cytoplasm are less distinct compared to bacteria located toward the periphery
of the lobule (Fig. 3A, B). (Note: sulfur deposits are identified as vacuoles where sulfur
was extracted during tissue dehydration and embedding procedures.) Bacteria located
toward the center of the lobule also appear smaller. Concentric membrane whorls
within the bacteria are occasionally visible (Fig. 4A, upper left).

Although it is difficult to fully trace eucaryotic cell membranes, the following evi-
dence indicates that the vacuole-enclosed bacteria are located within animal cells
(bacteriocytes). There are nuclei, mitochondria, and other organelles interspersed
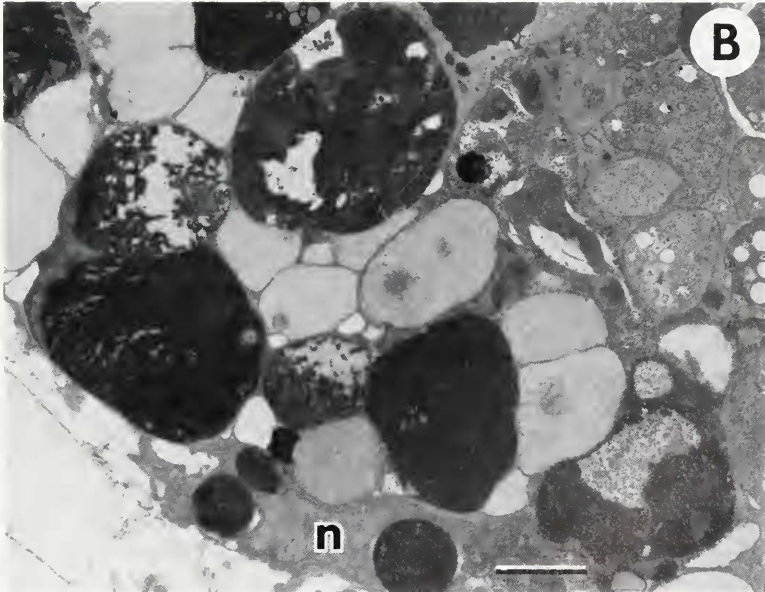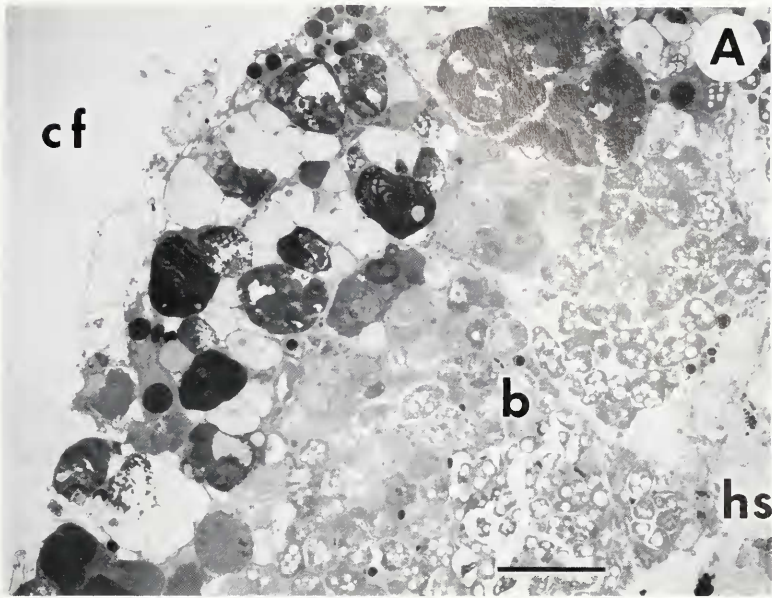among the bacteria (Fig. 4A, B). In Figure 4A, it is possible to delineate (moving

FIGURE 1.   A. Cross section of a trophosome lobule from *Riftia pachyptila* viewed at low magnification with transmission EM. The outer trophochrome cell layer contacts the coelomic fluid space (cf). Subtending this pigmented cell layer are numerous bacteria (b). At the center of the lobule is a hemolymph space (hs). Scale bar = 10 microns. B. Higher magnification of the trophochrome cells showing a nucleus (n) and the tight intracellular packaging of diverse types of granules. Scale bar = 3 microns.
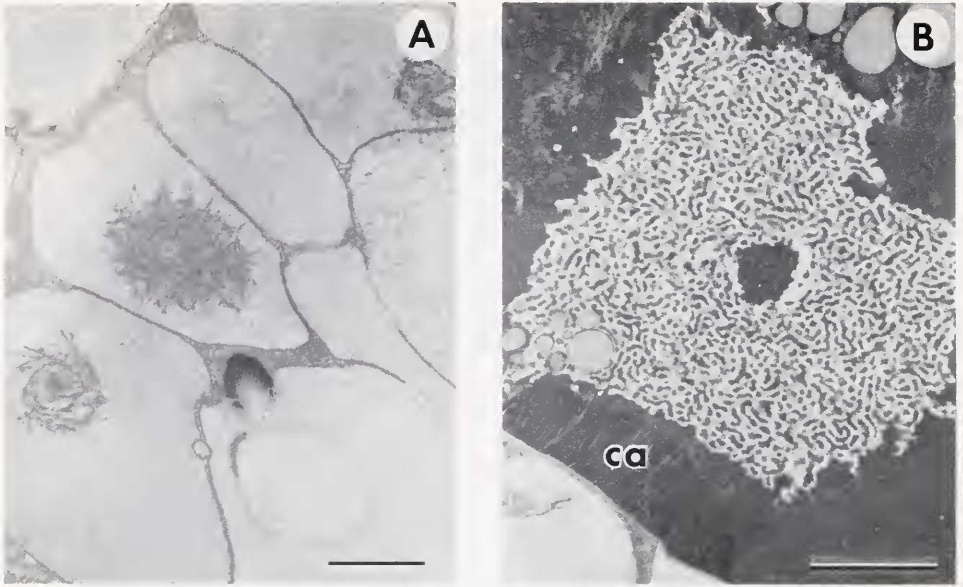
FIGURE 2. Two types of vacuole-enclosed granules present in trophochrome cells from *Riftia pachyptila*. A. Nondescript granules of uniform density, similar in appearance to mucigen granules. Scale bar = 1 micron. B. Electron-dense granule containing crystalline arrays (ca) of material that is proteinaceous in appearance. Scale bar = 2 microns.

outward from the center of the bacterium labeled "b") the bacterial cell envelope, the peribacterial membrane, and immediately adjacent, a nuclear envelope.

At the very center of the trophosome lobule, there is a hemolymph space or sinus extending longitudinally (Fig. 4B). We were unable to discern a basal lamina separating the bacteriocytes from the hemolymph space of the lobule.

Since the morphology and fine structure of the gill tissue from *C. magnifica* (Fiala-Medioni and Metivier, 1986) and *L. floridana* (Fisher and Hand, 1984) have already been described, we will not redescribe them here.

Isolated cell preparations

The cell purity for bacteriocytes isolated from bivalve gill tissue was approximately 70–80 percent (Table I). The amount of cellular debris present was not quantified, but was generally low. The yield of bacteriocytes was higher from *L. floridana* gill tissue than from *C. magnifica*. The reason may be that, while dissociation of *L. floridana* tissue was performed at 37°C, the incubation temperature for *C. magnifica* tissue had to be reduced to 20°C because of its temperature sensitivity. Although using 37°C incubations with the vent clam tissue improved the yield, the resulting bacteriocytes were not viable, as judged by the lack of ability to fix CO_2. Prior to the Percoll gradient step, the bacteriocytes represented 11% of the total cells in suspension from *L. floridana* gill. Thus, the density gradient fractionation achieved a 7-fold enrichment of bacteriocytes.

Attempts to isolate intact bacteriocytes from trophosome tissue were unsuccessful, suggesting that these cells are very fragile and are unable to withstand the isolation
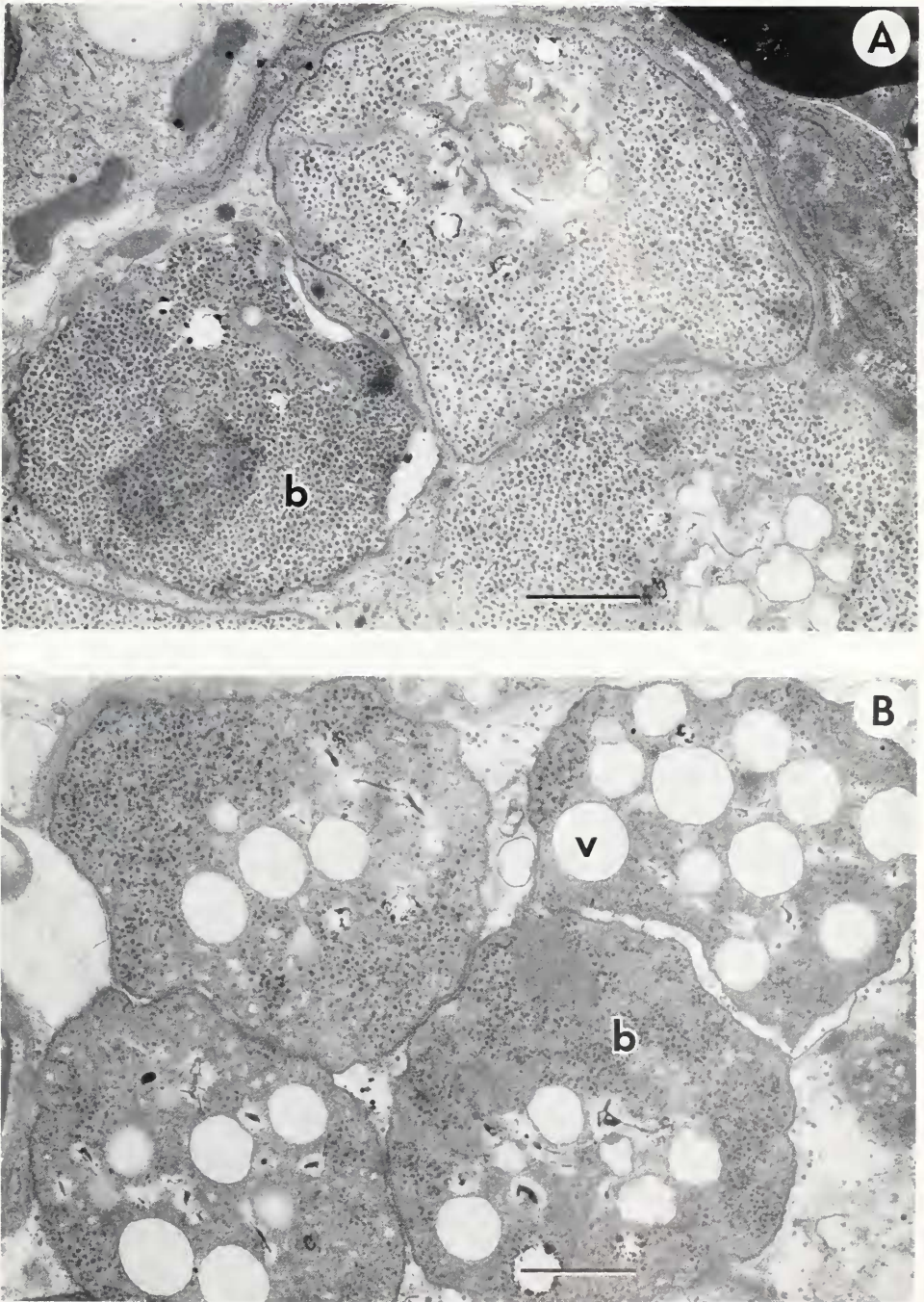
FIGURE 3. Bacteria (b) of *Riftia pachyptila* trophosome tissue. A. Located toward the periphery of the lobule, these bacteria are granular and contain very few sulfur deposits (observed as holes in the section where leaching has occurred). Scale bar = 1 micron. B. Bacteria located toward the center of the lobule contain more sulfur vacuoles (v), and their cytoplasm is less granular. Scale bar = 1 micron.
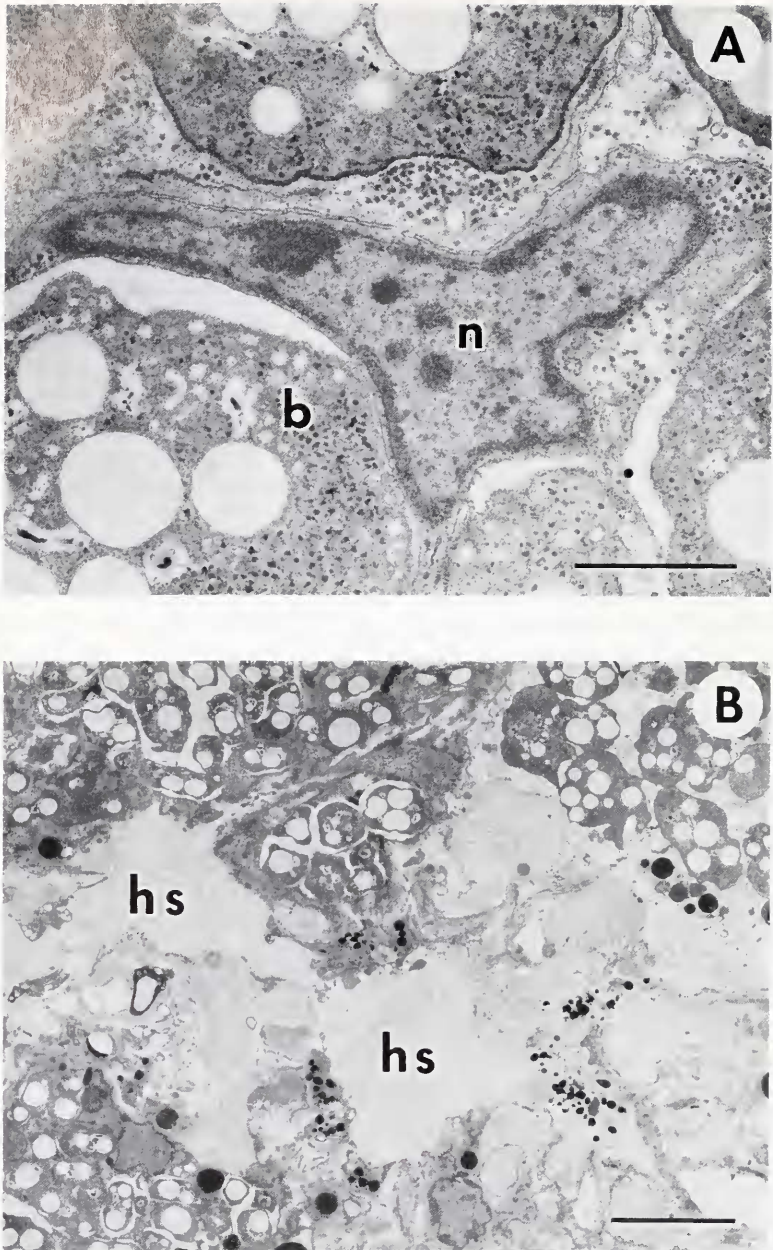
FIGURE 4. A. Bacterium (b) immediately adjacent to an animal cell nucleus (n). Scale bar = 1 micron. B. Micrograph showing hemolymph spaces (hs) located at the center of the lobule. Scale bar = 5 microns.

procedures. In contrast, trophochrome cells were enriched to a purity of 80%, and free bacteria were isolated in high yield and at a comparable purity to the pigmented trophosome cells. The primary contaminants of the trophochrome cell preparation were free bacteria.

TABLE 1

Yield and purity of isolated cell preparations

Cell source and type	Gradient interface (% Percoll)	Yield (million cells/g tissue)	Purity (% of total)	Protein (mg/million cells)
C. magnifica				
Bacteriocytes		1.16 ± 0.08[a]	72 ± 5.6	0.90 ± 0.14
	30–50%, 50–70%	(n = 3)	(n = 5)	(n = 3)
Non-bacteriocyte				
epithelial cells	10–30%	10.3	97	0.16
L. floridana				
Bacteriocytes	50–70%	3.0	81 ± 0.8	—
			(n = 3)	
R. pachyptila				
Bacteria	10–30%	—	79, 70	0.014
Trophochrome cells	30–50%, 50–70%	—	78, 82	1.09

[a] Mean ± standard error.

One prominent ultrastructural feature of isolated bacteriocytes from *C. magnifica* is wide-spread fields of bacteria—easily the most numerous subcellular structures in the cytoplasm (Figs. 5A, C; 6A). Compared to the bacteria present in trophosome tissue, these bacteria are much smaller (0.5–0.7 micron diameter). They are clearly contained in vacuoles within the bacteriocyte, and nuclear regions are evident (Fig. 6A).

Large granules (approximately 5–10 micron diameter) are a second salient feature of bacteriocytes from both *C. magnifica* (Fig. 5A, C) and *L. floridana* (Fig. 5B). Some of the *C. magnifica* granules are irregularly shaped and quite electron-dense, and others are more circular and have a stippled appearance. The electron-dense granules are morphologically similar to those of bacteriocytes from *L. floridana* (Fig. 5B, and Fisher and Hand, 1984). When viewed with Nomarski differential-interference-contrast microscopy, the granules of *L. Floridana* are striking and are certainly the dominant inclusion of the bacteriocyte (Fig. 5B). Previous work indicated the presence of iron in these granules (Fisher and Hand, 1984; *cf.*, Wittenberg, 1985), but whether the bacteriocytes' granules in *C. magnifica* are chemically similar is unknown. As judged by the sedimentation behavior of bacteriocyte populations in Percoll gradients, *L. floridana* bacteriocytes have a greater density, which may be a consequence of differences between these pigment granules. Bacteriocytes from *L. floridana* also are over two-fold larger in diameter than those from *C. magnifica* (Fig. 5A, B).

The morphology of isolated trophochrome cells (Fig. 6B) is essentially unchanged from that seen for intact tissue (Fig. 1B). On the other hand, isolated bacteria look more irregular in overall shape compared to those viewed *in situ* and occasionally were more vacuolated, suggesting that the isolation procedure for this cell type needs improvement.

Metabolic properties of isolated cells

The capacity for carbon dioxide fixation of *C. magnifica* bacteriocytes and isolated bacteria from *Riftia* trophosome is presented in Table II. In the absence of sulfur compounds, incorporation of CO_2 by bacteriocytes proceeds at a rate of 13 nmoles CO_2/mg protein/h. Fixation is inhibited by sulfide and, to a lesser degree, thiosulfate
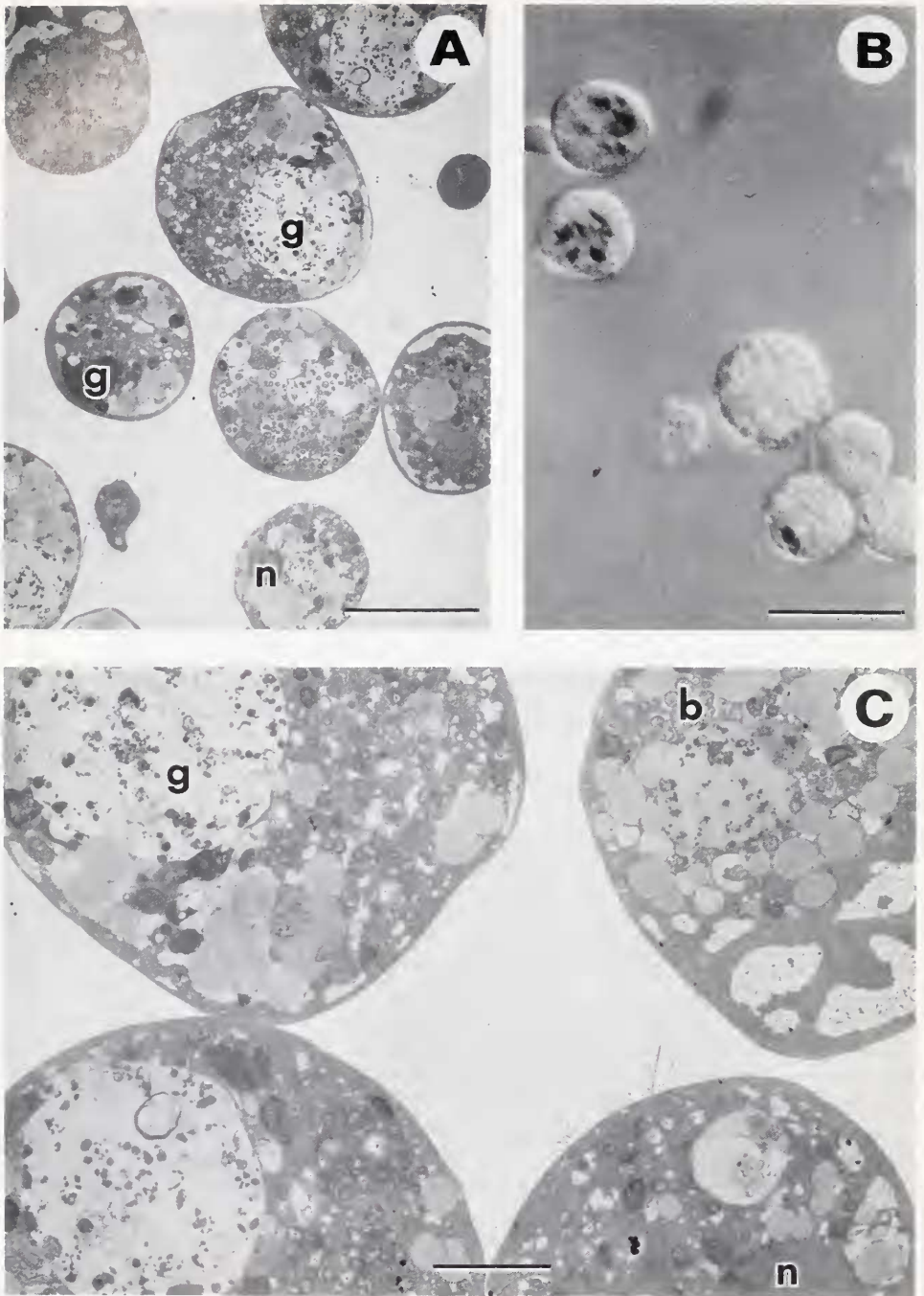
FIGURE 5.   A. Isolated bacteriocytes from the gill tissue of *Calyptogena magnifica* viewed with transmission EM. Two distinctly different granules (g) are observable in the cytoplasm. Scale bar = 15 microns. B. Nomarski light micrograph of bacteriocytes from *Lucina floridana* gill tissue, emphasizing the prominent granules in these very large cells. Scale bar = 60 microns. C. Higher magnification of *C. magnifica* bacteriocytes illustrating the expansive fields of symbiotic bacteria (b). Nucleus (n), granules (g). Scale bar = 5 microns.
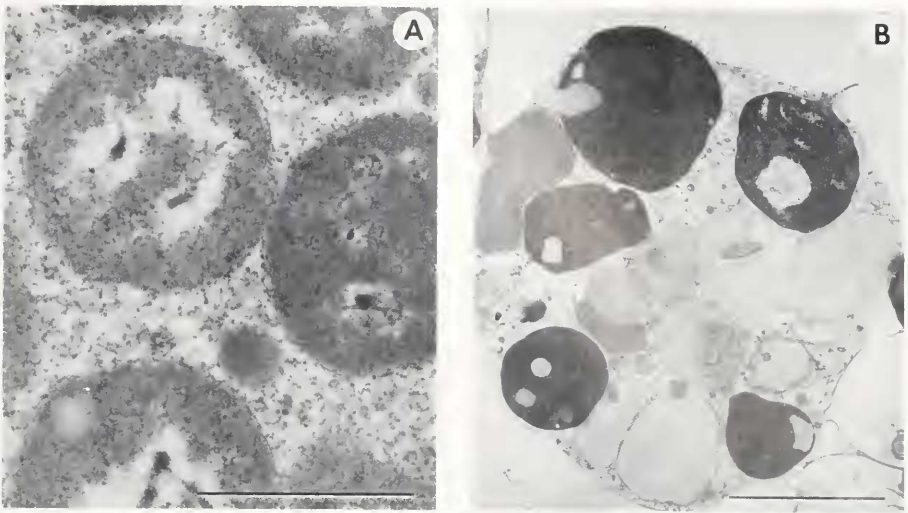
FIGURE 6.   A. High magnification (78,000 ×) of the symbiotic bacteria present in the cytoplasm of isolated bacteriocytes from *Calyptogena magnifica.* Note the peribacterial membrane encompassing each bacterium, and the distinct nuclear regions. The bacteria are approximately an order of magnitude smaller than those in *Riftia* trophosome. Scale bar = 0.5 micron. B. Isolated trophochrome cell from *Riftia pachyptila.* Scale bar = 5 microns.

across the range of concentrations used here. The rate of fixation by *L. floridana* bacteriocytes is approximately doubled by the addition of 0.1 mM thiosulfate; higher thiosulfate concentrations do not appreciably alter the fixation rate. Incorporation by non-bacteriocyte epithelial cells of *C. magnifica* is approximately one third the rate of *C. magnifica* bacteriocytes. The incorporation by the non-bacteriocyte preparation is presumably due to eucaryotic enzymes like pyruvate carboxylase and phosphoenolpyruvate carboxykinase, both known to occur in marine bivalves (*e.g.,* Felbeck, 1983; Meinardus-Hagar and Gäde, 1986). Contamination by bacteriocytes in this preparation is low (Table I).

The positive influence of sulfide on the intracellular ATP levels of *C. magnifica* bacteriocytes contrasts with the inhibitory effect seen on CO_2 fixation (Table III). After 60 min, bacteriocytes incubated in 0.5 mM sulfide contain 3.30 nmoles ATP/million cells (approximately 1.01 mM), compared to 1.02 nmoles/million cells (0.31 mM) with no added sulfur, and 1.74 nmoles/million cells (0.54 mM) with 0.5 mM thiosulfate.

DISCUSSION

The primary objectives of this study were (1) to describe ultrastructural features of *Riftia* trophosome tissue, particularly those related to the distribution and subcellular location of bacteria and the nature of the pigmented layer of trophochrome cells, (2) to prepare suspensions of isolated cells from invertebrate tissues that contain bacterial endosymbionts, and (3) to use these cellular preparations for characterizing metabolic aspects of the symbioses.

Morphological evidence supports the conclusion that symbiotic bacteria present in the trophosome of *R. pachyptila* are contained within animal cells (*i.e.,* bacterio-

S. C. HAND

TABLE II

Incorporation of carbon dioxide in isolated cell suspensions at 20°C

Preparation	Sulfur compound present	CPM/million cells/h	nmoles CO_2/ million cells/h	nmoles CO_2/ mg protein/h
C. magnifica				
Bacteriocytes	none	5632	13.9	13.0
		5976	14.8	13.3
	Na_2S: 0.1 mM	4590	11.4	—
		4272	10.6	9.5
	0.5 mM	3696	9.1	—
		4224	10.5	9.5
	1.0 mM	2676	6.6	—
	$Na_2S_2O_3$: 0.1 mM	4488	11.1	—
		5904	14.6	13.2
	0.5 mM	3084	7.6	
		3684	9.1	8.1
	1.0 mM	3792	9.4	8.4
Non-bacteriocyte epithelial cells	none	292	0.72	4.5
	Na_2S: 0.1 mM	404	0.10	6.2
	0.5 mM	302	0.75	4.6
	1.0 mM	318	0.79	4.8
	1.5 mM	348	0.86	5.3
	2.0 mM	136	0.34	2.1
	$Na_2S_2O_3$: 0.1 mM	292	0.72	4.5
	0.5 mM	266	0.66	4.0
	1.0 mM	246	0.61	3.8
	1.5 mM	274	0.68	4.2
	2.0 mM	292	0.72	2.2
L. floridana				
Bacteriocytes	none	3440	8.4	—
	$Na_2S_2O_3$: 0.1 mM	7776	19.0	—
	0.2 mM	7176	17.6	—
	0.5 mM	8728	21.4	—
	0.75 mM	7912	19.4	—
	1.0 mM	8824	21.6	—
R. pachyptila free bacteria	none	—	—	13.5

cytes). Electron micrographs show that nuclei and other eucaryotic organelles are frequently interspersed among the vacuole-enclosed bacteria, and eucaryotic cell membranes appear to enclose bacteria and such organelles within the same cell. Cavanaugh (1985) suggested that an intracellular location for the bacteria was probable, but previous evidence has been inconclusive (Cavanaugh *et al.,* 1981; Cavanaugh 1983, 1985).

A second notable point regarding trophosome fine structure is the distribution of sulfur deposits among the bacteria within a trophosome lobule. The bacteria located closer to the outer trophochrome layer clearly have fewer deposits than do bacteria located nearer the hemolymph space at the center of the lobule. This spatial distribution could reflect greater access of the latter bacteria to high sulfide concentrations in

TABLE III

Intracellular ATP levels of Calyptogena magnifica *bacteriocytes in the presence of sulfur compounds at 20°C*

Incubation time[1] (min)	Sulfur compound	nmoles ATP/ million cells	Calculated intracellular ATP concentration (mM)[2]
0	none	1.34	0.41
30	none	0.83	0.25
	0.5 mM Na$_2$S	1.34	0.41
	0.5 mM Na$_2$S$_2$O$_3$	0.88	0.28
60	none	1.02	0.31
	0.5 mM Na$_2$S	3.30	1.01
	0.5 mM Na$_2$S$_2$O$_3$	1.74	0.54
90	none	2.03	0.62
	0.5 mM Na$_2$S	3.75	1.15
	0.5 mM Na$_2$S$_2$O$_3$	1.29	0.40

[1] Cells were incubated at 20°C in artificial seawater (pH 8.2) containing the indicated concentrations of sulfide and thiosulfate.

[2] The intracellular concentrations of ATP were calculated using an average bacteriocyte diameter of 19.8 ± 0.8 microns (SE, n = 25), as determined from transmission electron micrographs. Cellular water content was assumed to be 80%.

Riftia vascular blood (Childress *et al.*, 1984). Indeed, Vetter (1985) showed that in the absence of sulfide, sulfur globules are lost from bacterial symbionts in the gill tissue of *Lucinoma annulata;* presumably the presence of sulfide would stimulate deposition of these elemental sulfur stores. The occurrence and possible roles of sulfur deposits in free-living sulfur bacteria recently have been reviewed (Vetter, 1985). It should be noted that the coelomic fluid of *Riftia* also contains sulfide, but it is unclear whether this sulfide pool is available directly to the symbionts, or must first be transferred to the vascular circulation (Childress *et al.*, 1984). If the density of sulfur deposits is related to the level of sulfur-based metabolism occurring in a given bacterium, then a gradient of metabolic activity could exist, with higher metabolic potential being possessed by bacteria closer to the central hemolymph space of the lobule. Bacteria near the hemolymph space also appear smaller, which is consistent with them being younger than the larger bacteria toward the outer trophochrome layer.

The morphology of the pigmented layer of trophosome tissue was far more complex than originally anticipated. First, the trophochrome layer does not contain bacterial endosymbionts, although the cells do contain extensive numbers of cytoplasmic inclusions (Figs. 1B, 2A, B). The function(s) of these cells is not understood presently, but their internal structure suggests several possibilities. Some of the intracellular droplets or granules are structurally similar to those found in mucus-secreting cells (*e.g.*, intestinal goblet cells). What benefit the secretion of mucus-like material (if it were to occur) by trophochrome cells would confer to the tubeworm is unclear, other than possibly lubricating the external surface of the trophosome that is in direct apposition to the internal surface of the body wall of the worm. Another possible function of trophochrome cells, that of phagocytosis and degradation of aging bacteria, is suggested by the heterogeneous contents of other intracellular granules (Fig. 1B). Future experiments measuring levels of protease activity in isolated trophochrome cells could be enlightening in this context. Finally, trophochrome cells also contain electron-dense material that is deposited as crystalline arrays in some granules (Fig. 4B).

This material is likely proteinaceous and may be the pigment responsible for the deep green color of the trophosome.

The region of the trophosome containing the bacteriocytes is a diffuse, loosely associated tissue, which suggests that its dissociation into suspensions of single bacteriocytes should have been relatively straight forward. Apparently however, the cells are very fragile, and we were unable to obtain intact bacteriocytes from trophosome even when mechanical agitation was kept to a minimum.

Thus, the isolated cellular preparation that may have the most potential for improving our understanding of the mechanisms involved in metabolic utilization of sulfur by the symbiosis is the bacteriocytes from *C. magnifica* and *L. floridana*. The ultrastructure of these isolated cells is comparable to the structure as viewed *in situ* (Fisher and Hand, 1984; Fiala-Medioni and Metivier, 1986), with the exception that bacteria in isolated bacteriocytes from *C. magnifica* appear a little more spherical than those in intact tissue (pers. obs., and Fiala-Medioni and Metivier, 1986). The size of *C. magnifica* bacteria differs markedly from those of *Riftia* trophosome, and data from 5S rRNA sequencing suggest the bacteria from the two sources have minimal affiliation (Stahl *et al.*, 1984; Lane *et al.*, 1985).

The temperature sensitivity of *C. magnifica* bacteriocytes closely parallels the observations of Belkin *et al.* (1986) in their studies with gill homogenates of the vent mussel *Bathymodiolus thermophilus*. In both cases, the capacity for CO_2 fixation declines dramatically at temperatures above 20°C. Thus, the bacterial endosymbionts from *C. magnifica* are comparable to those of *B. thermophilus* in that both appear to be sulfur-oxidizing bacteria with psychrophilic characteristics (*cf.*, Belkin *et al.*, 1986). The detrimental effect of warm temperature was not observed for bacteriocytes from the shallow-water bivalve *L. floridana*, and in general this cellular preparation seemed hardier.

In the absence of an exogenously added sulfur source, the rate of CO_2 fixation by *C. magnifica* bacteriocytes was 13 nmoles/mg protein/h. Rates obtained with homogenates of *B. thermophilus* gill ranged between 1.7 and 9.4 nmoles/mg protein/h, depending on temperature and the thiosulfate concentrations present (Belkin *et al.*, 1986). Using "purified" bacteria from *B. thermophilus*, Belkin *et al.*, (1986) reported maximum CO_2 fixation rates of approximately 40 nmoles/mg protein/h in the presence of thiosulfate. In the present study, CO_2 fixation by *C. magnifica* bacteriocytes was inhibited by sulfide across the range of 0.1 to 1.0 mM. Less inhibition was seen with thiosulfate. Similarly, Anderson (1986) showed that CO_2 fixation by whole specimens of *Solemya reidi* was inhibited at sulfide concentrations above 0.1 mM in surrounding seawater. This protobranch bivalve has a chemoautotrophic metabolism based on the presence of sulfur bacteria localized in its gill tissue (Felbeck, 1983). Unfortunately, we do not have measurements of CO_2 fixation by bacteriocytes at sulfide concentrations below 0.1 mM. Considering Anderson's results (1986), such sulfide levels could well stimulate the process.

CO_2 fixation by *L. floridana* bacteriocytes was increased approximately two-fold by thiosulfate concentrations between 0.1 and 1.0 mM, a pattern virtually identical to that seen for gill homogenates of *B. thermophilus* (Belkin *et al.*, 1986). Exogenously added sulfide was minimally effective in stimulating the process in *L. floridana* bacteriocytes (preliminary observations) and in *B. thermophilus* homogenates (Belkin *et al.*, 1986). The rate of CO_2 fixation by isolated bacteria from *R. pachyptila* trophosome was 13.5 nmoles/mg protein/h in the absence of added sulfur. The response to sulfide and thiosulfate was highly variable, and thus the results are not reported here. This variability could be related to the general instability of the CO_2 fixation capacity exhibited by trophosome preparations (Belkin *et al.*, 1986).

Although sulfide (0.1 mM and above) inhibited CO_2 fixation by isolated bacterio-cytes from *C. magnifica*, the presence of 0.5 mM sulfide promoted higher intracellu-lar ATP concentrations than control incubations without any added sulfur. The op-posing effects of sulfide on the two processes may be related to the sulfide concentra-tions used; as discussed earlier, if lower sulfide levels had been tried, CO_2 fixation might also have been stimulated. Thiosulfate was not as effective in enhancing intra-cellular ATP levels. Powell and Somero (1986a), using lysed bacterial preparations from *C. magnifica* gill, showed that sulfite stimulated ATP synthesis while thiosulfate and sulfide did not. In their study, ATP was measured using the firefly luciferase technique, and incubations were of shorter duration. Most likely, components of the animal cell contributed to sulfide utilization in our study with isolated bacteriocytes. Although some degree of spontaneous oxidation is possible, Powell and Somero (1985) localized sulfide oxidizing bodies in the animal cell cytoplasm of *S. reidi* gill tissue. These workers also have conclusively demonstrated that mitochondria iso-lated from *Solemya reidi* gill tissue can couple sulfide oxidation to the formation of ATP via the electron transport system and oxidative phosphorylation (Powell and Somero, 1986b).

Thus, the initial step(s) of sulfide oxidation could occur in bacteriocytes prior to the sulfur compound reaching the endosymbiont, and some of the ATP synthesis in bacteriocytes could reflect mitochondrial processing. Consequently, the identities of sulfur compounds exploited for chemical energy by the symbiosis may depend on the structural organization and integrity of the biological preparation under study. Additional metabolic characteristics of invertebrate-sulfur bacteria symbioses may display similar dependencies in ways yet to be identified.

LITERATURE CITED

ANDERSON. A. E. 1986. Autotrophy and the relationship of CO_2, O_2, and sulfide flux in the bacterial symbiont-containing clam *Solemya reidi. Am. Zool.* **26**(4): 58A.
ARP, A. J., J. J. CHILDRESS, AND C. R. FISHER, JR. 1984. Metabolic and blood gas transport characteristics of the hydrothermal vent bivalve *Calyptogena magnifica. Physiol. Zool.* **57**: 648–662.
BELKIN, S. D., D. C. NELSON, AND H. W. JANNASCH. 1986. Symbiotic assimilation of CO_2 in two hydro-thermal vent animals, the mussel *Bathymodiolus thermophilus,* and the tube worm, *Riftia pa-chyptila. Biol. Bull.* **170**: 110–121.
CAVANAUGH, C. M. 1983. Symbiotic chemoautotrophic bacteria in sulfide-habitat marine invertebrates. *Nature* **302**: 58–61.
CAVANAUGH, C. M. 1985. Symbiosis of chemoautotrophic bacteria and marine invertebrates from hydro-thermal vents and reducing sediments. *Bull. Biol. Soc. Wash.* **1985**(6): 373–388.

Cavanaugh, C. M., S. L. Gardiner, M. L. Jones, H. W. Jannasch, and J. B. Waterbury. 1981. Prokaryotic cells in the hydrothermal vent tube worm, *Riftia pachyptila:* possible chemoautotrophic symbionts. *Science* **213:** 340–342.

Childress, J. J., A. J. Arp, and C. R. Fisher, Jr. 1984. Metabolic and blood characteristics of the hydrothermal vent tube-worm, *Riftia pachyptila. Mar. Biol.* **83:** 109–124.

Childress, J. J., and T. J. Mickel. 1980. A motion compensated shipboard precision balance system. *Deep-Sea Res.* **27A:** 965–970.

Dando, P. R., A. J. Southward, E. C. Southward, N. B. Terwilliger, and R. C. Terwilliger. 1985. Sulphur-oxidising bacteria and haemoglobin in gills of the bivalve *Myrtea spinifera. Mar. Ecol. Prog. Ser.* **23:** 85–98.

Felbeck, H. 1981. Chemoautotrophic potential of the hydrothermal vent tube worm *Riftia pachyptila* Jones (Vestimentifeera). *Science* **213:** 340–342.

Felbeck, H., J. J. Childress, and G. N. Somero. 1981. Calvin-Benson cycle and sulphide oxidation enzymes in animals from sulphide-rich habitats. *Nature* **293:** 291–293.

Felbeck, H. 1983. Sulfide oxidation and carbon fixation by the gutless clam *Solemya reidi:* an animal-bacteria symbiosis. *J. Comp. Physiol. B* **152:** 3–11.

Felbeck, H. 1985. CO_2 fixation in the hydrothermal vent tube worm *Riftia pachyptila* (Jones). *Physiol. Zool.* **58**(3): 272–281.

Fiala-Medioni, A., A. M. Alayse, and G. Cahet. 1986. Evidence of *in situ* uptake and incorporation of bicarbonate and amino acids by a hydrothermal vent mussel. *J. Exp. Mar. Biol. Ecol.* **96:** 191–198.

Fiala-Medioni, A., and C. Metivier. 1986. Ultrastructure of the gill of the hydrothermal vent bivalve *Calyptogena magnifica,* with a discussion of its nutrition. *Mar. Biol.* **90:** 215–222.

Fisher, C. R., Jr., and J. J. Childress. 1984. Substrate oxidation by trophosome tissue from *Riftia pachyptila* Jones (Phylum Pogonophora). *Mar. Biol. Lett.* **5:** 171–183.

Fisher, M. R., and S. C. Hand. 1984. Chemoautotrophic symbionts in the bivalve *Lucina floridana* from seagrass beds. *Biol. Bull.* **167:** 445–459.

Hand, S. C., and G. N. Somero. 1983. Energy metabolism pathways of hydrothermal vent animals: adaptations to a food-rich and sulfide-rich deep sea environment. *Biol. Bull.* **165:** 167–181.

Hessler, R. R., and W. Smithey. 1983. The distribution and community structure of megafauna at the Galapagos rift hydrothermal vents. *NATO Conf. Ser. (Mar. Sci.)* **12:** 735–770.

Lane, D. J., D. A. Stahl, G. J. Olson, and N. R. Pace. 1985. Analysis of hydrothermal vent-associated symbionts by ribosomal RNA sequences. *Bull. Biol. Soc. Wash.* **1985**(6): 389–400.

Lowry, O. H., and J. V. Passonneau. 1972. *A Flexible System of Enzymatic Analysis.* Academic Press, New York. 291 pp.

Meinardus-Hager, G., and G. Gäde. 1986. The pyruvate branchpoint in the anaerobic energy metabolism of the jumping cockle *Cardium tuberculatum* L.: D-lactate formation during environmental anaerobiosis versus octopine formation during exercise. *Exp. Biol.* **45:** 91–110.

Peterson, G. L. 1977. A simplification of the protein assay method of Lowry *et al.* which is generally more applicable. *Anal. Biochem.* **83:** 346–356.

Porter, K. R., and M. A. Bonneville. 1973. *Fine Structure of Cells and Tissues.* Lea and Febiger, Philadelphia. 204 pp.

Powell, M. A., and G. N. Somero. 1983. Blood components prevent sulfide poisoning of respiration of the hydrothermal vent tube worm *Riftia pachyptila. Science* **219:** 297–299.

Powell, M. A., and G. N. Somero. 1985. Sulfide oxidation occurs in the animal tissue of the gutless clam, *Solemya reidi. Biol. Bull.* **169:** 164–181.

Powell, M. A., and G. N. Somero. 1986a. Adaptations to sulfide by hydrothermal vent animals: sites and mechanisms of detoxification and metabolism. *Biol. Bull.* **171:** 274–290.

Powell, M. A., and G. N. Somero. 1986b. Hydrogen sulfide oxidation is coupled to oxidative phosphorylation in mitochondria of *Solemya reidi. Science* **233:** 563–566.

Stahl, D. A., D. J. Lane, G. J. Olsen, and N. R. Pace. 1984: Analysis of hydrothermal vent-associated symbionts by ribosomal RNA sequences. *Science* **224:** 409–411.

Vetter, R. D. 1985. Elemental sulfur in the gills of three species of clams containing chemoautotrophic symbiotic bacteria: a possible inorganic energy storage compound. *Mar. Biol.* **88:** 33–42.

Wittenberg, J. B. 1985. Oxygen supply to intracellular bacterial symbionts. *Bull. Biol. Soc. Wash. D.C.* **1985**(6): 301–310.